

## Supplementary Information

Matrix-free dynamic nuclear polarization enables solid-state NMR  $^{13}\text{C}$ – $^{13}\text{C}$   
correlation spectroscopy of proteins at natural isotopic abundance

Hiroki Takahashi, Sabine Hediger and Gaël De Paëpe\*

*Laboratoire de Chimie Inorganique et Biologique, UMR-E3 (CEA/UJF) and CNRS, Institut Nanosciences  
et Cryogénie, CEA, 38054 Grenoble, France*

\*Corresponding author: Gaël De Paëpe (Email: [gael.depaepe@cea.fr](mailto:gael.depaepe@cea.fr))

## **Table of Contents**

Section 1: DNP-enhanced SSNMR at high fields

Section 2: Water content in the MF sample

Section 3: Experimental conditions

Section 4: Sample preparation

Section 5: Optimization of decay times

Section 6: Figures S1 – S6

References

## Section S1: DNP-enhanced SSNMR at high fields

### Introduction

Dynamic nuclear polarization (DNP) is a technique employed to enhance the sensitivity of NMR by utilizing the larger polarization of electron spins ( $\gamma_e/\gamma_H = 660$ ,  $\gamma$ : gyromagnetic ratio) which is transferred to nuclear spins.<sup>1-4</sup> DNP at a high field ( $> 5$  T) requires a high-power ( $\sim 5$  W) and high-frequency (e.g. 263 GHz at 9.4 T) microwave source (gyrotron) to saturate electron spins.<sup>5-7</sup> Generated microwaves are efficiently transmitted from the microwave source using corrugated waveguides<sup>7</sup> or quasi-optical transmission<sup>8</sup> to the sample located in a low-temperature magic-angle-spinning (MAS) probe. Samples are generally doped with polarizing agents such as TOTAPOL<sup>9</sup> and bTbK<sup>10</sup>. Griffin and co-workers demonstrated DNP experiments at 5 T in the 1990's<sup>5,11</sup> and the applicable magnetic field has since been extended up to 16.4 T<sup>12</sup>. DNP enhancement depends on various factors such as the sample temperature and the magnetic field. Typical DNP enhancement factors ( $\varepsilon_{\text{DNP}}$ ) in <sup>13</sup>C-CPMAS experiments using TOTAPOL have been reported to be 20 – 80 on small organic molecules<sup>7,13</sup> and 20 – 30 on membrane proteins<sup>14,15</sup> at  $\sim 100$  K and 9.4 T.

### Absolute Sensitivity Ratio (ASR)<sup>16</sup>

$\varepsilon_{\text{DNP}}$  is measured by comparing spectra recorded under the same conditions with and without microwave irradiation. Other factors such as signal bleaching, linewidths, changes in relaxation times, etc. also contribute to a signal-to-noise ratio (S/N) per unit time either positively or negatively and need to be considered when performing DNP experiments.

The absolute sensitivity ratio (ASR) has been introduced to evaluate an effective DNP enhancement, which is experimentally determined by comparing the S/N per unit time in a DNP experiment and a conventional solid-state NMR (SSNMR) experiment. The ASR can be rationalized by eight different factors that contribute to an effective DNP enhancement positively/negatively as follows:

$$\text{ASR} = \varepsilon_{\text{DNP}} \cdot \varepsilon_{\text{T}} \cdot \eta_{\text{TI}} \cdot \chi_{\text{bleach}} \cdot \chi_{\text{LW}} \cdot \chi_{\text{weight}} \cdot \chi_{\text{seq}} \cdot \chi_{\text{ex}} \quad (1)$$

with

$\varepsilon_T$  : the sensitivity gain at low temperature (increase of magnetization according to the Boltzmann distribution and the reduction of thermal noise). In theory,  $\varepsilon_T = (T_{RT}/T_{DNP})^{3/2}$  where  $T_{RT}$  and  $T_{DNP}$  are the temperatures used for the conventional SSNMR at room temperature and the DNP experiment at low temperature, respectively. DNP experiments performed at 105 K can then gain a maximum enhancement factor of  $(298 \text{ K}/105 \text{ K})^{3/2} = 4.78$  from  $\varepsilon_T$ .

$\eta_{T1}$  : a square root of the ratio of repetition times for DNP and conventional SSNMR experiments,  $\eta_{T1} = (T_{1,conv}/\tau_{DNP})^{1/2}$  where  $T_{1,conv}$  and  $\tau_{DNP}$  are the longitudinal relaxation time constant for the conventional SSNMR experiment and the DNP build-up time constant in the DNP experiment, respectively.

$\chi_{bleach}$  : the ratio of the detectable spins between the samples with and without polarizing agents.

$\chi_{LW}$  : the ratio of the apparent linewidths between the DNP and conventional NMR experiments.

$\chi_{weight}$  : the ratio of the effective sample weights between the DNP and conventional NMR samples.

$\chi_{seq}$  : the ratio of the effective magnetization between the DNP and conventional NMR experiments after decays that are pulse sequence specific. This usually depends on  $T_{1\rho}$  (rotating-frame longitudinal relaxation time constant under continuous RF field) and/or  $T_2'$  (transverse dephasing time constant during a spin-echo).

$\chi_{ex}$  : the factor caused by extra effects (e.g. when using a different probe, magnetic field, etc.).

### ***Matrix-Free DNP***

In DNP experiments, samples of interest are usually dissolved or suspended in glass-forming matrices (containing water and cryo-protectant, such as glycerol or DMSO) doped with polarizing agents in order to achieve uniform radical distribution around the sample of interest. However, the use of glassy matrices significantly reduces the effective amount of sample ( $\chi_{weight} < 1$ ). The use of glass-forming matrices also causes spectral line-broadening due to the conformational distribution in frozen solutions

( $\chi_{\text{LW}} < 1$ ). Inorganic materials are usually robust against this type of line-broadening but for organic compounds this can be a severe limitation.

In order to optimize  $\chi_{\text{weight}}$  and  $\chi_{\text{LW}}$  for MAS-DNP experiments, we introduced a matrix-free (MF) approach where the polarizing agents are uniformly distributed in the sample without using glass-forming matrices. This approach maximizes the effective quantity of material observed. Also, line-broadening caused by conformational distribution at low temperatures can be avoided or minimized if ordered solids are used. The two main strategies to perform MF-DNP experiments are described in the article.

## **Section S2: Water content in the MF sample**

The water content in the MF lysozyme sample was measured and compared to that in the sample prepared by a conventional sample-packing method using centrifugation. The MF lysozyme sample was prepared by the procedure described in Section 4. The conventional lysozyme sample was prepared by centrifuging a mixture of crystalline lysozyme with its mother liquor (containing Tris buffer and NaCl) for three minutes (12,000 *g*). Then the supernatant was removed. The weights of these samples were 104.7 mg and 119.1 mg for the MF sample and the conventional sample, respectively. They were dried in a desiccator under vacuum for ca. 24 hours. The final weights were 61.6 mg and 46.1 mg which corresponds to a water content of 43.1 mg (41%) and 73.0 mg (61%) in the MF sample and the conventional sample, respectively. Although the MF sample contains 41% water by mass (not by volume), which is important to retain crystal structures and achieve efficient DNP enhancements, it does not contain too much bulk water and thus the sample density is much higher. The MF sample is packed in a NMR rotor in the same way as powdered samples.

As seen above, the MF lysozyme sample contains 41% water by mass. This water plays an important role to retain crystal structures and achieve better packing and efficient DNP enhancements. This is different from a 'DNP matrix' that is used for uniform distribution of polarizing agents at low temperature. The MF approach achieves uniform distribution of polarizing agents using direct or indirect binding affinities of polarizing agents to the sample of interest. There is no 'DNP matrix' in the MF sample in this respect.

### Section S3: Experimental conditions

All DNP experiments were performed on a Bruker AVANCE III 400 MHz NMR system equipped with a 263 GHz fundamental mode gyrotron, a transmission line (corrugated waveguides) and a low temperature (~100 K) triple resonance 3.2-mm MAS probe.<sup>7</sup> The data were recorded, processed and analyzed using Bruker Topspin 3.0. The sample temperature was 105 K and MAS frequencies are specified in the figure captions. For 1D <sup>13</sup>C-CPMAS experiments (see Figure S1 for the pulse sequence), 100 kHz of RF-field strength was applied for the <sup>1</sup>H  $\pi/2$  pulse and SPINAL-64 heteronuclear decoupling<sup>17</sup>. The <sup>13</sup>C CP spin-lock was applied at a RF-field strength of 60 kHz and the <sup>1</sup>H RF-field strength was adjusted to match a Hartmann-Hahn condition using a linear ramp. The CP contact time was set to 1 ms. The time-domain signals were zero-filled and Fourier transformed without any apodization.

The pulse sequence used for the 2D <sup>13</sup>C homonuclear dipolar correlation experiments involving the SPC5 recoupling scheme<sup>18</sup> is shown in Figure S1. The same <sup>1</sup>H RF-field strength as for the 1D <sup>13</sup>C-CPMAS experiments were used for  $\pi/2$  pulse and SPINAL-64 decoupling. The MAS frequency was set to 10.5 kHz. The <sup>13</sup>C RF-field strength during SPC5 recoupling was 52.5 kHz. High-power <sup>1</sup>H Lee-Goldburg<sup>19</sup> continuous wave (CW) decoupling was applied during the recoupling pulses. The SPC5 recoupling times for Figs. 3 and S6 were set to 1.52 ms ( $n = 4$ ) and 4.57 ms ( $n = 12$ ), respectively. Recycle delays, the numbers of scans and the numbers of complex  $t_1$  points (spectral width: 52.5 kHz) were 2.5 s, 112 and 48 (0.91 ms evolution time) for Fig. 3, and 4.0 s, 256 and 48 for Fig. S6. Quadrature detection in the indirect dimension was obtained by States-TPPI. Forward linear prediction for an additional 80 points was used in the indirect dimension. Experimental data were zero-filled and apodized with 60 Hz and 200 Hz of exponential line-broadening in the direct and indirect dimensions, respectively, for Fig. 3 (100 Hz and 200 Hz for Fig. S6) prior to Fourier transformation.

1D <sup>13</sup>C-CPMAS experiments using conventional SSNMR were performed on a Bruker AVANCE 400 MHz NMR system with a double-resonance 4-mm MAS probe at room temperature. All RF-field strengths and processing parameters used were the same as for the 1D DNP-enhanced NMR experiments.

#### **Section S4: Sample preparation**

The biradical TOTAPOL was synthesized according to the literature.<sup>9</sup>

*Adenosine and glycine samples:* adenosine and glycine were purchased from Sigma-Aldrich (Lyon, France). Adenosine (50 mg) was first dissolved in 200  $\mu$ L of 1,1,1,3,3,3-hexafluoro-2-propanol (HFIP), and then precipitated by slowly adding methanol (500  $\mu$ L); all performed in an ultrasonic bath. The sample was centrifuged and the supernatant was removed. D<sub>2</sub>O (200  $\mu$ L) solution containing TOTAPOL (0.16 mg), glucose (3.6 mg) and glycerol (4 mg) was added to the sample which was then dried in a desiccator under vacuum. Glycine (50 mg) was dissolved in H<sub>2</sub>O (1.5 mL) with glucose (3.6 mg) and TOTAPOL (0.80 mg). This solution was spread in the form of 10  $\mu$ L droplets on a Petri dish and dried in a desiccator under vacuum. The obtained samples were fully packed into 3.2-mm thin-wall zirconia rotors.

*Lysozyme sample:* lysozyme from chicken egg white was purchased from Sigma-Aldrich (Lyon, France). We prepared two DNP samples with different TOTAPOL concentrations and NMR relaxation times (see Section 5 for further details). Lysozyme sample used for Figs. 2 (b) and 3 (DNP build-up time ( $\tau_{\text{DNP}}$ ) of 1.9 s): lysozyme (150 mg) was dissolved in H<sub>2</sub>O (3mL). To this solution, 1.5 M NaCl in 50 mM Tris buffer (pH 7.0, 6 mL) containing trehalose (10.8 mg) and TOTAPOL (1.9 mg) was added. The solution was partially evaporated in a desiccator under vacuum and the precipitate then collected by centrifugation. H<sub>2</sub>O (30  $\mu$ L) containing trehalose (3.6 mg), glycerol (2 mg) and TOTAPOL (0.48 mg) was added to the sample, which was then dried in a desiccator under vacuum. 54 mg of the product was packed into a 3.2-mm thin-wall zirconia rotor. Lysozyme sample used for Fig. S6 ( $\tau_{\text{DNP}}$  of 3.1 s): lysozyme (150 mg) was dissolved in H<sub>2</sub>O (3mL). To this solution, 1.0 M NaCl in 50 mM Tris buffer (pH 7.0, 6 mL) containing trehalose (10.8 mg) and TOTAPOL (0.80 mg) was added. The solution was partially evaporated in a desiccator under vacuum and the precipitate was collected by centrifugation. H<sub>2</sub>O (50  $\mu$ L) containing trehalose (1.8 mg), glycerol (1 mg) and TOTAPOL (0.32 mg) was added to the sample, which was then dried in a desiccator under vacuum. 50 mg of the product was packed into a 3.2-

mm thin-wall zirconia rotor.

### **Section S5: Optimization of decay times**

Pulse sequences that contain long spin-locking, refocused evolution or polarization exchange periods suffer from signal decay depending on  $T_{1\rho}$ ,  $T_2'$ , etc., especially so in the presence of paramagnetic spins. This decay affects  $\chi_{\text{seq}}$  in Eq. (1) and as a consequence, reduces the ASR. Therefore, it is often important to measure decay times at certain radical concentrations. Figure S5 shows  $T_2'$  decay curves for the lysozyme samples containing two different TOTAPOL concentrations. Although  $T_2'$  is not directly relevant to the decay during SPC5 recoupling periods, it gives a relative estimation of the decay under the presence of paramagnetic spins. We used the lysozyme sample that possesses the shorter decay time (and accordingly, recycle time) for the experiment with the shorter recoupling period and the sample with the longer-lived magnetization for the longer-recoupling experiment.

Section S6: Figures S1 – S6

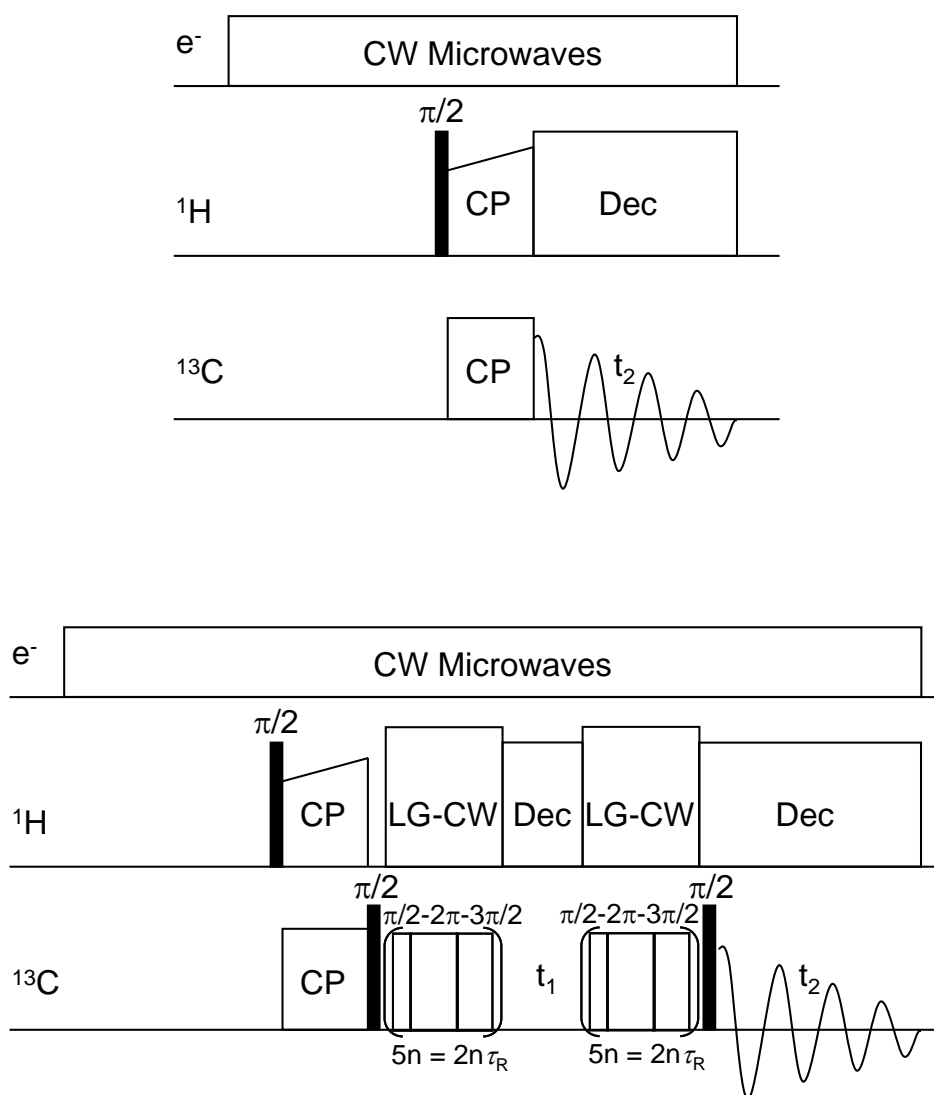


**Figure S1.** Pulse sequences used to record DNP-enhanced 1D  $^{13}\text{C}$ -CPMAS (top) and 2D DQ-SQ SPC5 (bottom) spectra. Electron spins are saturated throughout the experiments by CW microwave irradiation which leads to the DNP enhancement of  $^1\text{H}$  magnetization further used by a standard NMR pulse sequence.

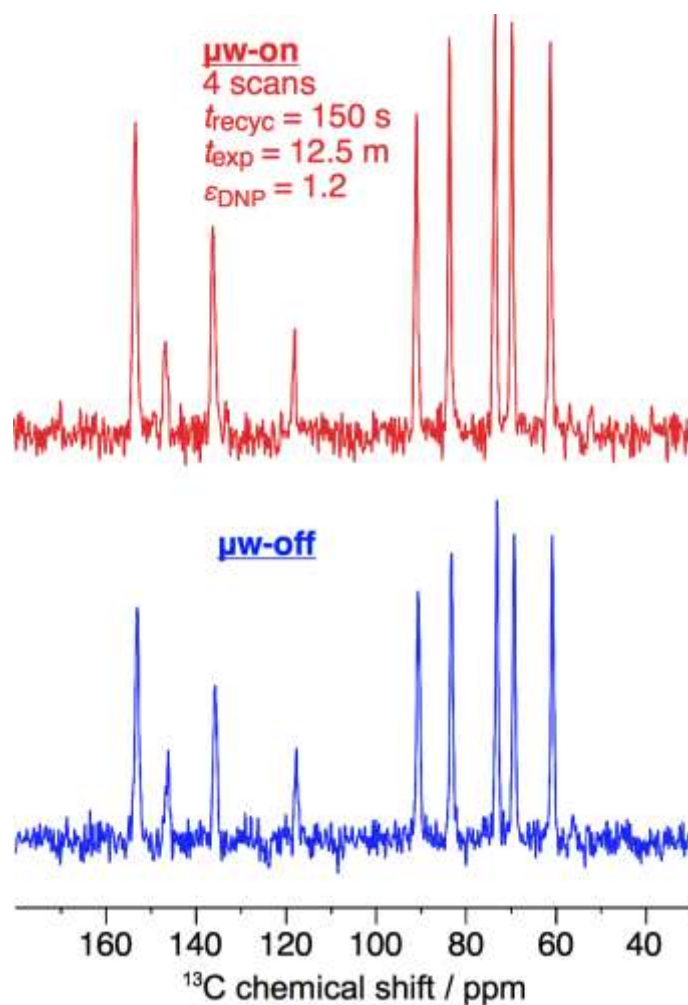


**Figure S2.** 1D  $^{13}\text{C}$ -CPMAS spectra with microwaves-on (top) and -off (bottom) of a matrix-free adenosine sample doped with TOTAPOL but without a gluing agent. The MAS frequency was 8 kHz. The absence of significant DNP enhancement ( $\epsilon_{\text{DNP}} = 1.2$ ) and the longer DNP build-up time constant ( $> 200$  s) suggest that TOTAPOL is not uniformly distributed around the sample.

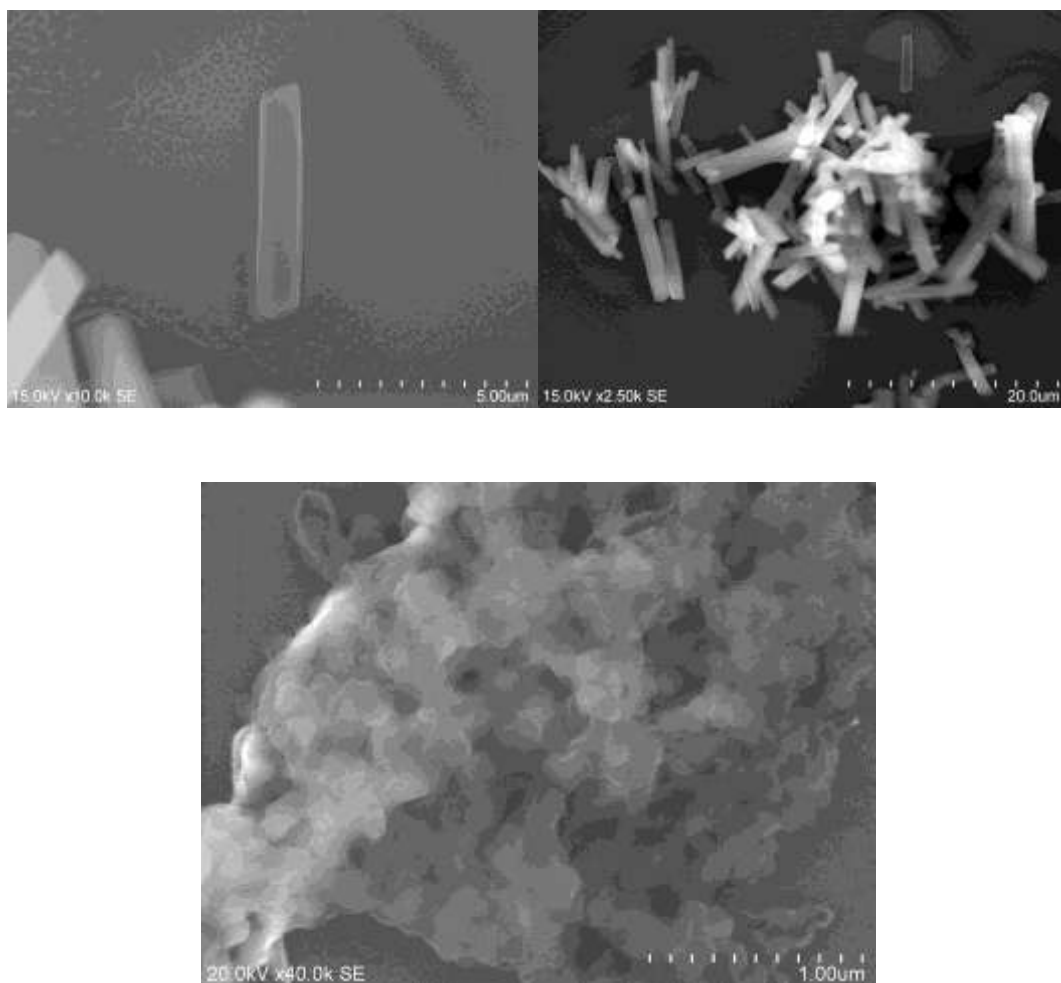


**Figure S3.** SEM images of recrystallized adenosine (top) and lysozyme (bottom). The size of the obtained adenosine crystals is typically a few  $\mu\text{m}$  in width and 5 – 20  $\mu\text{m}$  in length. According to the image, small lysozyme crystallites ( $< 100$  nm) aggregate and form large objects after the removal of solvents.

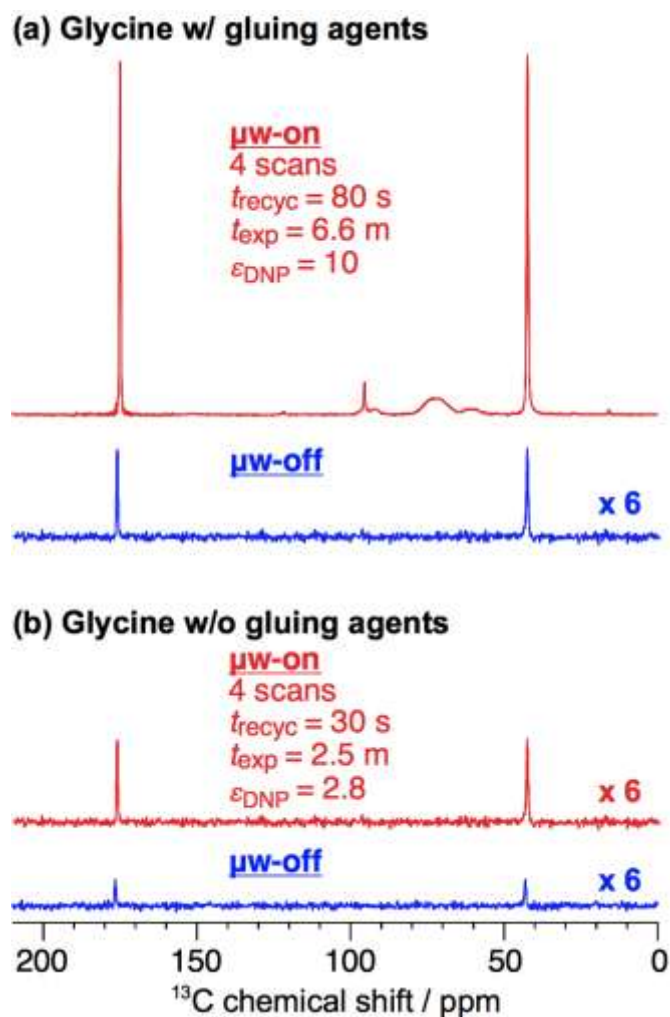


**Figure S4.** 1D  $^{13}\text{C}$ -CPMAS spectra of a matrix-free glycine sample doped with TOTAPOL together with (a) and without (b) gluing agents (glucose), recorded with microwaves-on and -off. The MAS frequency was 8 kHz. Moderate enhancement ( $\epsilon_{\text{DNP}} = 10$ ) was seen using gluing agents, whereas very low DNP enhancement ( $\epsilon_{\text{DNP}} = 2.8$ ) was obtained without gluing agents. This also supports the principle that glucose acts as a gluing agent. Reduction of the crystal size will help to obtain even larger DNP enhancements.

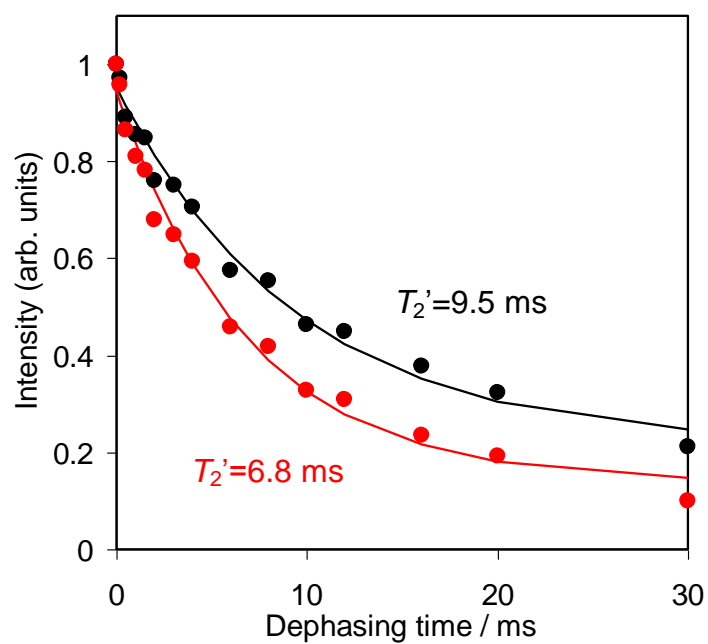


**Figure S5.** Refocused transverse  $^{13}\text{C}$  magnetization decays of the MF-DNP lysozyme samples with lower TOTAPOL concentration (black) and higher concentration (red).

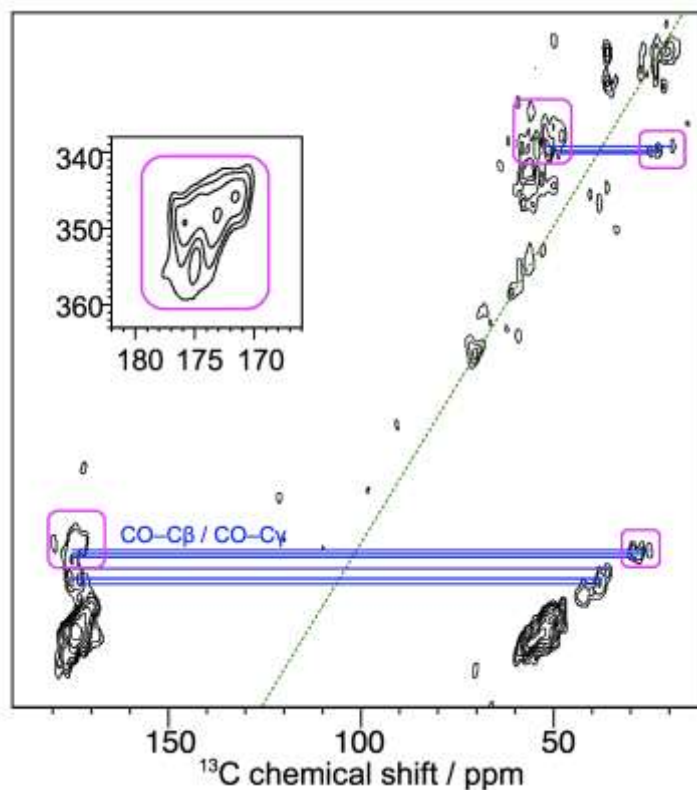


**Figure S6.** A DNP-enhanced 2D DQ-SQ  $^{13}\text{C}$ - $^{13}\text{C}$  dipolar correlation spectrum of natural-abundance lysozyme prepared by the MF method. The MAS frequency was 10.5 kHz and the SPC5 recoupling time was 4.57 ms. For other experimental conditions, see Section 3. New peaks appearing, compared to the shorter recoupling time experiment (Figure 3), are marked in magenta. DQ: double quantum, SQ: single quantum.

## **References**

1. Overhauser, A. W. *Phys. Rev.* **92**, 411–415 (1953).
2. Carver, T. R. & Slichter, C. P. *Phys. Rev.* **92**, 212–213 (1953).
3. Carver, T. P. & Slichter, C. P. *Phys. Rev.* **102**, 975–980 (1956).
4. Abragam, A. & Goldman, M. *Rep. Prog. Phys.* **41**, 395–467 (1978).
5. Becerra, L. R., Gerfen, G. J., Temkin, R. J., Singel, D. J. & Griffin, R. G. *Phys. Rev. Lett.* **71**, 3561–3564 (1993).
6. Bajaj, V. S., Farrar, C. T., Hornstein, M. K., Mastovsky, I., Viereg, J., Bryant, J., Elena, B., Kreisler, K. E., Temkin, R. J. & Griffin, R. G. *J. Magn. Reson.* **160**, 85–90 (2003).
7. Rosay, M., Tometich, L., Pawsey, S., Bader, R., Schauwecker, R., Blank, M., Borchard, P. M., Cauffman, S. R., Felch, K. L., Weber, R. T., Temkin, R. J., Griffin, R. G. & Maas, W. E. *Phys. Chem. Chem. Phys.* **12**, 5850–5860 (2010).
8. Pike, K. J., Kemp, T. F., Takahashi, H., Day, R., Howes, A. P., Kryukov, E. V., MacDonald, J. F., Collis, A. E. C., Bolton, D. R., Wylde, R. J., Orwick, M., Kosuga, K., Clark, A. J., Idehara, T., Watts, A., Smith, G. M., Newton, M. E., Dupree, R. & Smith, M. E. *J. Magn. Reson.* **215**, 1–9 (2012).
9. Song, C., Hu, K. N., Joo, C. G., Swager, T. M. & Griffin, R. G. *J. Am. Chem. Soc.* **128**, 11385–11390 (2006).
10. Matsuki, Y., Maly, T., Ouari, O., Karoui, H., Le Moigne, F., Rizzato, E., Lyubenova, S., Herzfeld, J., Prisner, T., Tordo, P. & Griffin, R. G. *Angew. Chem. Int. Ed.* **48**, 4996–5000 (2009).
11. Hall, D. A., Maus, D. C., Gerfen, G. J., Inati, S. J., Becerra, L. R., Dahlquist, F. W. & Griffin, R. G. *Science* **276**, 930–932 (1997).
12. Barnes, A. B., Markhasin, E., Daviso, E., Michaelis, V. K., Nanni, E. A., Jawla, S. K., Mena, E. L., DeRocher, R., Thakkar, A., Woskov, P. P., Herzfeld, J., Temkin, R. J. & Griffin, R. G. *J. Magn. Reson.* **224**, 1–7 (2012).
13. Lange, S., Linden, A. H., Akbey, U., Franks, W. T., Loening, N. M., van Rossum, B. J. & Oschkinat, H. *J. Magn. Reson.* **216**, 209–212 (2012).

14. Linden, A. H., Lange, S., Franks, W. T., Akbey, U., Specker, E., van Rossum, B. J. & Oschkinat, H. *J. Am. Chem. Soc.* **133**, 19266–19269 (2011).
15. Jacso, T., Franks, W. T., Rose, H., Fink, U., Broecker, J., Keller, S., Oschkinat, H. & Reif, B. *Angew. Chem. Int. Ed.* **51**, 432–435 (2012).
16. Takahashi, H., Lee, D., Dubois, L., Bardet, M., Hediger, S. & De Paëpe, G. *Angew. Chem. Int. Ed.* **51**, 11766–11769 (2012).
17. Fung, B. M., Khitrin, A. K. & Ermolaev, K. *J. Magn. Reson.* **142**, 97–101 (2000).
18. Hohwy, M., Rienstra, C.M., Jaroniec, C.P. & Griffin, R.G. *J. Chem. Phys.* **110**, 7983–7992 (1999).
19. Lee, M. & Goldberg, W. I. *Phys. Rev. A*, **140**, 1261–1271 (1965).